Research & Reviews: Journal of Chemistry e-ISSN: 2319-9849

Fluorescence Resonance Energy Transfer Biosensor Based on Nitrogen Doped Carbon Quantum Dots and Hairpin Probe to Sensitively Detect Aflatoxin Biosynthesis-Related Genes aflD in Rice

Qingyue Sun[1], Dezhao Kong[1], Chang Liu[1], Qiaoqiao Shi[1], Tao Yu[2], Shuangfeng Peng[2], Yaqi Li[1,3,4*], Yong Chen[4]

[1]Department of Chemical Engineering, Jiangsu University of Science and Technology, Zhenjiang, China
[2]Department of Environmental Engineering, Jiangsu University of Science and Technology, Zhenjiang, China
[3]Department of Advanced Technology, Jiangsu University of Science and Technology, Zhenjiang, China
[4]Department of Environmental Science, Huazhong University of Science and Technology, Wuhan, China

Research Article

Received: 17-Mar-2023, Manuscript No. JCHEM-23-92057; **Editor assigned:** 20-Mar-2023, PreQC No. JCHEM-23-92057(PQ); **Reviewed:** 03-Apr-2023, QC No. JCHEM-23-92057; **Revised:** 10-Apr-2023, Manuscript No. JCHEM-23-92057(R); **Published:** 17-Apr-2023, DOI: 10.4172/2319-9849.12.1.005

***For Correspondence:**
Yaqi Li, Department of Chemical Engineering, Jiangsu University of Science and Technology, Zhenjiang, China
E-mail: liyaqi@just.edu.cn

Citation: Sun Q, et al. Fluorescence Resonance Energy Transfer Biosensor Based on Nitrogen Doped Carbon Quantum Dots and Hairpin Probe to Sensitively Detect

ABSTRACT

The expression of aflD gene plays a significant role in the biosynthesis of aflatoxin, aflD structural genes can be served as a good biomarker of aflatoxigenic strains. The detection of the aflD gene is a promising method to control the further spread of aflatoxins. In this research, a rapid fluorescence biosensor targeting aflatoxigenic biosynthesis-related genes aflD was developed based on Nitrogen-doped Carbon Quantum Dots (NCQDs) and AuNPs (Gold nanoparticles) as fluorescence donors and quenchers respectively. This sensor was fabricated by immobilization of NCQDs and AuNPs on the two ends of hairpin DNA. In the absence of the aflD gene, NCQDs were closed to AuNPs to trigger the fluorescence resonance energy transfer leading to a quenching and showed the fluorescent signal "off". In the presence of the aflD gene, NCQDs and AuNPs were separated by the target aflD gene complementary matching with the loop of the hairpin structure, which caused to the recovery of fluorescence signal and performance the fluorescent signal "on". It was shown that the biosensor provided an excellent Limit of Detection (LOD) of 1.95 nM (3 σ /k) with a liner range of 10 nM-150 nM. Besides, this biosensor performed the satisfied selectivity through the comparison between aflD gene and mismatched DNA sequences. The feasibility of this biosensor was examined in rice contaminated by *Aspergillus flavus*. Therefore, it could potentially be used as a feasible tool for preventing aflatoxin in grain and its products.

Keywords: aflD gene; *Aspergillus flavus*; Biosensor; Fluorescence; Aflatoxigenic;

Aflatoxin Biosynthesis-Related Genes aflD in Rice. RRJ Chemist. 2023;12:005.

Contaminated; Sequences

INTRODUCTION

Aflatoxins (AFs) are mycotoxins produced by certain species of *Aspergillus* that grow on a wide variety of crops, mainly cereals [1]. Aflatoxins can contaminate most food and feed crops, which occur frequently in maize, groundnut, rice [2,3]. They are related to some diseases such as emesis, edema, tumor induction and teratogenesis [4]. Meanwhile, according to the data of FAO, 25% of global agricultural products are contaminated by mycotoxins every year, causing hundreds of billions of dollars in financial losses [5]. aflD is one of the structural genes of aflatoxin gene cluster in *Aspergillus flavus* and other *Aspergillus spp*. aflD gene can encode an enzyme with a molecular weight of 29 KD, which play a significant role in producing aflatoxins [6]. Therefore, it can indicate that the aflD gene has the potential to be a biomarker of aflatoxins [7].

Development of the food productions increases the risk of the food contamination with the microbial or chemical agents. Although several methods have been developed to detect this microorganism, an effective strategy for presenting this toxigenic fungus has not been shown yet [8]. DNA biosensors have extremely potential functions, especially for the food analyses as an emerging and developed application [9,10]. In comparison to other methods, fluorescent biosensors due to sensitivity, simplicity, repeatability, portability, and compatibility with the microfabrication technologies are the widely accepted detection platforms for DNA analyses [11-15]. In these methods, labeled fluorescence nanomaterials biosensors have widely applied for the detection of aflatoxins owing to their direct sample determination, high specificity, rapid signal response [16,17]. Compared with the immunosorbent assay, the DNA biosensor exhibited the excellent stability. To obtain high sensitivity, the hairpin DNA was used to construct Foster Resonance Energy Transfer (FRET) detection strategy [18]. FRET is a non-radiative energy transfer phenomenon through long-range dipole-dipole interactions between donors and acceptors [19]. FRET system can be influenced by three crucial elements including the distance between fluorescent acceptor and donor molecules, degree of spectral overlap and dipole orientation of donor and acceptor [20,21]. FRET has been considerably used in fluorescence sensing probes, such as in drug release, biological analysis, and heavy metal ions assay [22,23].

Fluorescence donor-acceptor pair is the one of critical factors in the construction of a molecular beacons systems. Organic fluorescent dyes are widely used in traditional molecular beacons system, due to they possess good

stability, outstanding quantum yield and convenient chemical modification. However, it still existed some shortcomings including photobleaching, unity of dye color and biological toxicity restrict their application of molecular beacons [24]. Therefore, more and more scientists started to devote the research of Quantum Dots (QDs) owning remarkable fluorescence properties and intended to replace the organic dyes by QDs to achieve the low toxicity and photobleaching resistance. Carbon Dots (CDs) are carbon particles with fluorescent properties smaller than 10 nm in size [25]. Nitrogen doping can significantly improve the fluorescence properties of quantum dots. Nitrogen-doped Carbon Quantum Dots (NCQDs) can make up for some defects of traditional probes modified by organic dyes and have become a promising substitution to organic dyes because of their unique characteristics including excellent thermo/photostability, high quantum yield, low toxicity, small sizes, good biocompatibility and low cost [26,27]. At present, nanomaterials with excellent fluorescence quenching efficiency through FRET are regarded as the fascinating substrates to alternate traditional organic quenchers in many fluorescence biosensors [28]. There are some FRET donor-acceptor pairs reported such as CdTe QDs-AuNPs, Graphene QDs-Cerium oxide nanoparticles, FAM-MXene and AuNCs- polydopamine nanospheres [29-31]. Therefore, nanomaterials can be used as a proficient approach to construct fluorescence probes.

In this work, NCQDs and AuNPs were firstly synthesized by hydrothermal and one-step reduction respectively, which exhibited excellent fluorescence and UV-vis absorbance properties respectively. Account of the mode of FRET between NCQDs and AuNPs, a detection system for sensitive and specific aflD gene determination was established. This assay was constructed by hairpin DNA probe modified NCQDs and AuNPs at both ends of hairpin DNA. In the absence of the aflD gene, the NCQDs can be closed to AuNPs; the fluorescence of the NCQDs was quenched by AuNPs through FRET. In the presence of the aflD gene, the loop of the hairpin probe was reorganized, the fluorescent signal was recovered in varying degrees accordingly to obtain the purpose of quantitative determination aflD gene under preferred conditions. This method exhibited high sensitivity, repeatability, and credibility. Besides, this designed FRET hairpin probe switch was used in the detection of real rice samples and obtained a good result, which showed this method had the potential ability to be a feasible instrument for the aflD gene determination in the food pollution.

MATERIALS AND METHODS

Material and reagents

All chemicals were of analytical reagent grade and used as purchased without further treatment. Citric acid ($C_6H_8O_7{\cdot}H_2O$, ≥ 99.5%), Ethylenediamine, Tris(2-carboxyethyl) phosphine hydrochloride (TCEP), Tris-HCl, 1-Ethyl-3-(3-dimethyllaminopropyl) carbodiimide hydrochloride (EDC), and N-hydroxysuccinimide (NHS), 2-(N-morpholino) ethanesulfonic acid, $HAuCl_4{\cdot}4H_2O$ (47.8%) and sodium citrate [32]. All the DNA oligonucleotides utilized in this work were provided and purified by Sangon (Shanghai, China). The DNA sequences were heated to 95°C for 10 minutes and then cooled to room temperature for at least 6 hours for later use. The detailed sequences information for all the DNAs were shown in Table 1. Rice samples were randomly collected from local markets in Zhenjiang (Jiangsu Province, PR China). They were purchased in their original packages (10 kg). The category of rice is the nanjing 9108.

Table1. The sequence of DNA information.

Name	Sequence (from 5'-3')
tDNA	GGATCTCAACTCCCCTGGTAG
Hairpin DNA	H_2N-CGGCCGCTACCAGGGGAGTTGAGATCCCGGCCG-SH
5 Mismatched DNA	GTATCTGAACTGCCATGGTAG
2 Mismatched DNA	GGATGTCAACTCCGCTGGTAG
DNA	CTGCATGTAGTAATGCCACGT

Apparatus

All fluorescence Random spectra of the samples were obtained on spectrofluorometer FS5. The UV-visible absorption spectra were measured on a Shimadzu UV-3600 spectrophotometer. Data were collected in the wavelength range of 200 nm-800 nm. The size and topography of AuNPs were characterized by Transmission Electron Microscopy (TEM) (JEM-1400plus Japan). Fourier Transform Infrared (FT-IR) measurement was carried out with a Tensor-27 FT-IR spectrometer (Bruker Co., Germany). X-ray Diffraction (XRD) spectra of NCQDs were acquired by using a Bruker D8 ADVANCE powder X-ray diffractometer (Karlsruhe, Germany). Elemental and functional groups analysis is performed on an ESCALAB 250 X-ray photoelectron spectrometer (XPS, AXIS-Ultra DLD).

Synthesis of NCQDs

The NCQDs were prepared according to the reported work [11]. 1.05 g of citric acid and 335 µl of ethylenediamine were dispersed in 20 ml of ultrapure water. Then the solution was poured into a poly (tetrafluoroethylene) (Teflon)-lined autoclave (50 ml) and reacted at 200°C for 5 hours. After the reaction, the reactors were cooled to room temperature naturally. The product, which was filtered by 0.22 µm microporous membrane, was dialysed for 24 hours by a 1000 Da dialysis bag and placed at 4°C for later use.

Preparation of AuNPs

AuNPs with the average size of 16 nm were synthesized by one-step reduction of $HAuCl_4$ with sodium citrate in solution [33]. Before the experiment, all-glass instruments were soaked in aqua regia for 12 hours, cleaned with ultrapure water, and dried. The detailed process was as follows: 50 ml of $HAuCl_4$ (1 mM) was added to a three-necked flask, heated to boiling, and refluxed under magnetic stirring, and then 5 ml of sodium citrate solution (1.0 wt%) was quickly injected. The color of the solution quickly changed from light yellow to wine, and continued to reflux for 10 minutes. The solution cooled to room temperature naturally, was filtered by 0.22 µm microporous membrane, and stored at 4°C for later use.

Functionalization of AuNPs and NCQDs with thiol-modified Hairpin DNA

For the coupling process for the AuNPs-hairpin DNA referred to the report by Liu, et al. work [34]. Briefly, the thiol-modified hairpin DNA was incubated with freshly prepared TCEP (10 mM) at room temperature for 1 hour. 960 µl of AuNPs were transferred to 40 µl of TCEP-treated thiol hairpin DNA (10 µM) with gentle shaking for 24 hours at 37°C, 53 µl of PB buffer solution (0.2 M) was added to the above solution, incubating for 12 hours at 37°C. In the same interval, making the final concentration of NaCl solution is 0.2 M by adding 2 M NaCl solution, then the

solution was incubated at 37°C for another 24 hours. The final sample was centrifuged at 10,000 rpm for 10 minutes 3 times with 500 µl of Tris-HCl (10 mM, pH 8.0), and dispersed in 200 µl of Tris-HCl (10 mM, PH 8.0) buffer solution with a volume fraction of 0.02% Tween-20 for the later use.

The hairpin DNA probe was coupled with the surface of NCQDs according to the previous work [35]. Firstly, the prepared NCQDs were redispersed in 5 ml of MES buffer (PH 6) solution, and then 19 mg EDC and 22 mg NHS were added to the NCQDs solution and stirred at room temperature for 1 hour to activate the carboxyl functional groups on the surface of the NCQDs. Then, the pH value of the NCQDs solution was adjusted to 7, and AuNPs-Hairpin DNA was incubated with the above solution for the night at 37°C. The final solution was centrifuged at 10,000 rpm for 5 minutes 3 times with Tris-HCl buffer and the hairpin probe was gained by redispersing the precipitation in the Tris-HCl buffer solution.

RESULTS AND DISCUSSION

The principle and feasibility of DNA fluorescence biosensors

Supplementary Figures 1-3 exhibited the principle for the determination of the aflD gene based on the NCQDs and AuNPs FRET. Firstly, NCQDs and AuNPs were coupled to 5' and 3' ends of Hairpin DNA through amido and Au-S bonds. In the absence of the aflD gene, NCQDs were closed to AuNPs. At this time, fluorescence resonance energy transfer was occurred between NCQDs and AuNPs, so that the fluorescence emitted by the NCQDs were absorbed by the AuNPs and radiated in the form of heat, so that the fluorescence of the NCQDs was quenched. In the presence of the aflD gene, NCQDs and AuNPs were integrated, the original Hairpin structure was destroyed, which led to the recovery of fluorescence signal. Therefore, the detection of the aflD gene can be achieved through the quenching and recovery of NCQDs fluorescence. Besides, by adjusting the appropriately corresponding target substance recognition sequence, this method could realize the detection of a variety of target substances. To test the feasibility of the proposed means, we chose gel electrophoresis to prove the successful combination of Hairpin DNA and the aflD gene. As is illustrated in the picture Supplementary Figure 1, it can be observed that the molecular weight of hairpin DNA increases significantly after aflD gene and Hairpin DNA is successfully combined. The above results showed that the FRET fluorescence sensing method based on NCQDs and AuNPs was feasible for aflD gene detection.

Characterization of NCQDs, AuNPs and hairpin probe

We firstly characterized our prepared NCQDs and AuNPs. According to the previous report, we successfully synthesized NCQDs and AuNPs [11,33]. Supplementary Figure 2A shows high-resolution transmission electron microscopy (TEM) images of the NCQDs, which can be seen to have a uniform dispersion without apparent aggregation and particle diameters of 2.22 nm. Well-resolved lattice fringes with an interplanar spacing of 0.212 nm were observed (Supplementary Figure 2B), which is close to the (100) facet of graphite. It can be observed that the obtained AuNPs with excellent solubility and dispersibility in water have an approximately spherical shape with a diameter of 16.68 nm (Figure 1A).

Figure 1B represented the characteristic peaks of NCQDs. The peak at 3250 cm^{-1} results from the stretching vibration of C-OH, and the stretching vibration peak of C-H and C=O appears at 2700 cm^{-1} and 1650 cm^{-1} respectively, which verified the existence of considerable polar functional groups such as hydroxyl and carboxyl groups on the surface of NCQDs. The peaks at 1080 cm^{-1} and 1550 cm^{-1} were ascribed to the asymmetric stretching vibrations of C-NH-C and N-H, demonstrating that the surface of NCQDs successfully combined with

amino groups. What's more, the relationship of groups was verified XPS analysis (Figures 1C-1F). Figure 1C showed the XPS full spectra of NCQDs exhibited three representative peaks at 285.58 eV, 399.58 eV and 533.58 eV, which corresponding to C1s, N1s and O1s. The high-resolution C1s spectra in Figure 1D exhibited four peaks at 284.9, 286.1 and 287.7 eV, corresponding to C=C/C-C, C-NH-C, and C=O groups respectively. The high-resolution N1s spectra of NCQDs in Figure 1E depicted one peaks at 399.8 eV, which were attributed to N-H and N-C. The O1s spectra of NCQDs in Figure 1F presented two peaks at 530.9 and 531.2 eV, which were assigned to O-H and O=C-O groups.

Figure 1A. Shows the TEM image of the AuNPs.

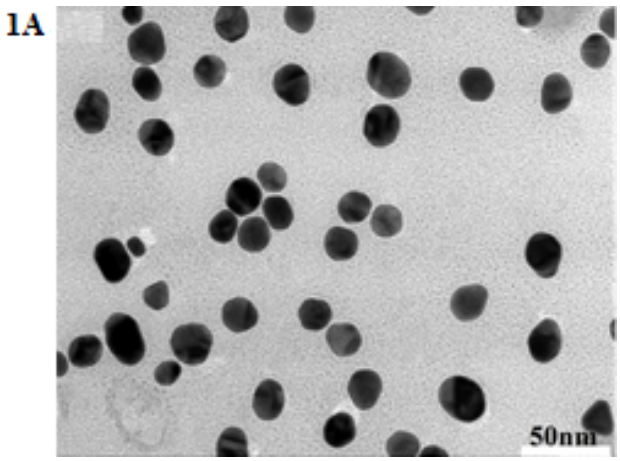

Figure 1B. Shows the FTIR spectra of NCQDs.

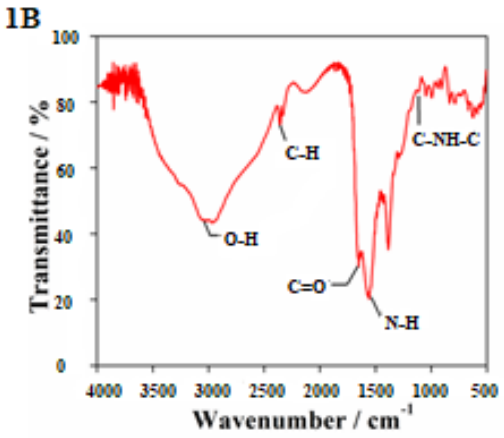

Figure 1C. Shows the NCQDs XPS full spectrum.

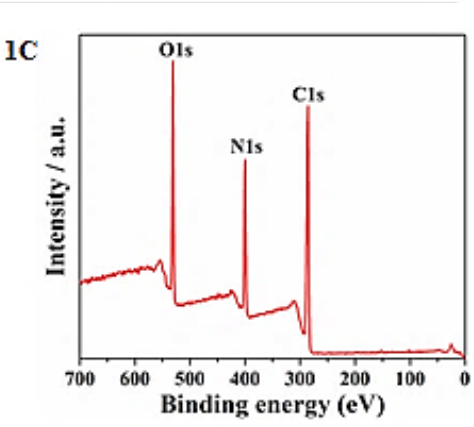

Figure 1D. Shows the NCQDs high-resolution spectra of C1s. **Note:** 284.9 eV(C-C,C=C); 286.1 eV(C-N); 287.7 eV(C=O).

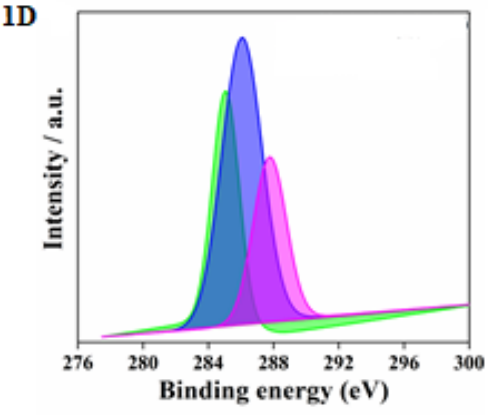

Figure 1E. Shows the NCQDs high-resolution spectra of N1s. **Note:** 399.8 eV(-NH,N-C).

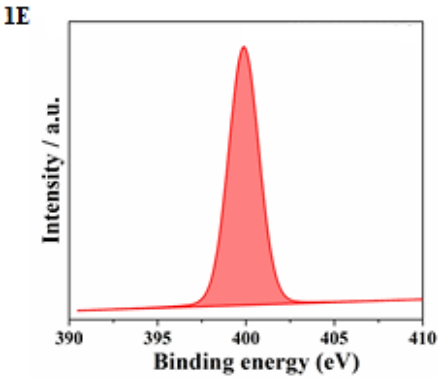

Figure 1F. Shows the NCQDs high-resolution spectra of O1s. **Note:** 530.9 eV(O-H); 531.2 eV(O=C-O).

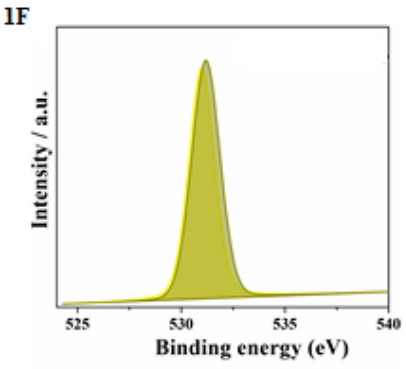

Figure 2A showed a broad peak concentrated at 24°C, which was also put down to highly unordered carbon atoms. The peak was mainly centralized on 241 nm and 350 nm in the UV/Vis spectra. The former was given rise to the π - π^* transition in C=C, and the latter was contributed to the n- π^* transition in -COOH and -NH_2, which is closely related to the fluorescence characteristics of NCQDs. In the fluorescence spectrum, the strongest fluorescence emission was situated at 445 nm when excited at 344 nm, and the NCQDs exhibited yellow and blue fluorescence under light (left in the inset) and UV lamp (right in the inset) (Figure 2B). The excitation-dependent photoluminescence behaviour was investigated Figure 2C, the emission wavelength of the NCQDs did not shift

depending on the excitation wavelength, which was connected with the fewer surface defects and uniform size of NCQDs. Thus, it showed that the obtained NCQDs had uniform morphology and abundant surface functional groups [36].

The UV-visible absorption spectra of NCQDs, AuNPs, and AuNPs-Hairpin DNA-NCQDs were investigated. Compared with AuNPs, the absorption spectra of AuNPs-Hairpin DNA-CQDs mildly shifted to the right after surface modification with Hairpin DNA, and a characteristic peak of DNA appeared at 260 nm, which was put down to the successful coupling of AuNPs and Hairpin DNA (Figure 2D) [37]. Compared with NCQDs, AuNPs-Hairpin DNA-NCQDs had stronger absorption at 241 nm and 350 nm. The strong absorption was attributed to the amide coupling of NCQDs and Hairpin DNA (Figure 2D).

Figure 2A. Shows the XRD of NCQDs.

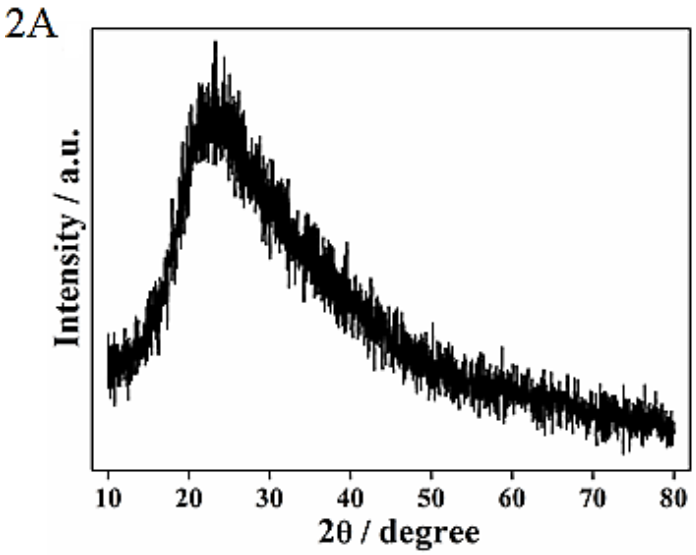

Figure 2B. UV/vis absorption (black curve), pl excitation (red curve), and emission spectra (blue curve) of NCQDs in aqueous solutions. Insets show photographs of NCQDs in aqueous solution under visible (left) and UV light (right).

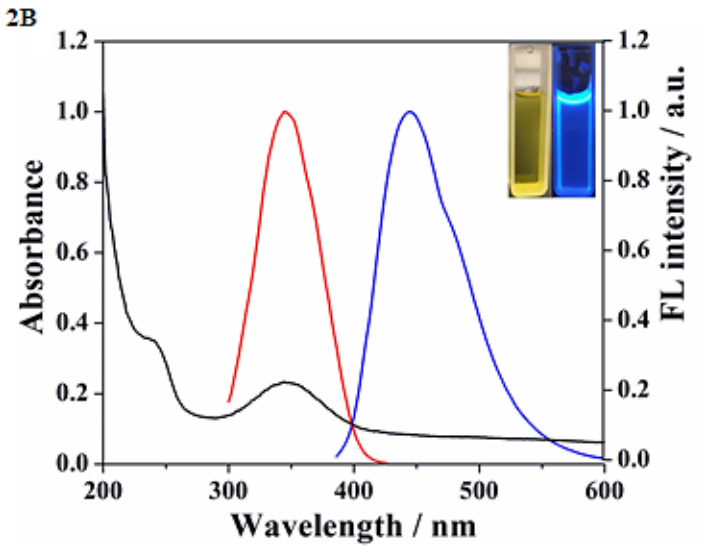

Figure 2C. PI of NCQDs at the different excitation wavelengths. **Note:** 300 nm; 320 nm; 340 nm; 360 nm; 380 nm; 400 nm.

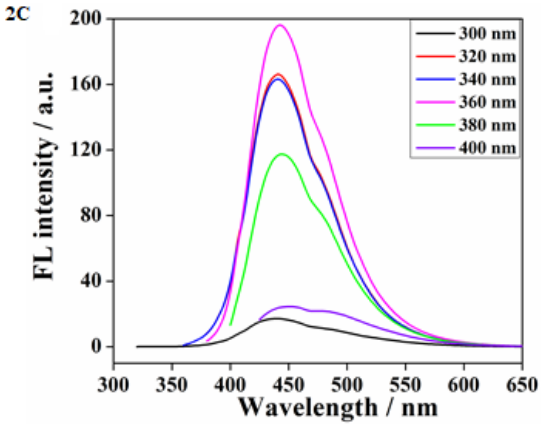

Figure 2D. UV-vis spectra of NCQDs, AuNPs and NCQDs-HP-AuNPs. **Note:** NCQDs; AuNPs; NCQDs-HP-AuNPs.

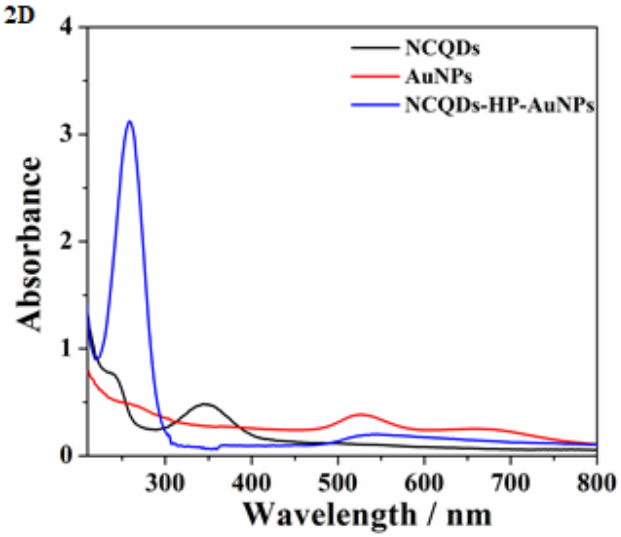

Optimization of working environment

To achieve a better analytical performance of this method, we separately investigated the impacts of hybridization temperature, incubation time, and buffer solution in the reaction on the quantum dots fluorescent biosensing platform. As shown in Figure 3A, it was found that the fluorescence reaches the maximum at 40°C, and the fluorescence intensity remains unchanged after increasing the temperature. The reaction time was another important parameter that affects the reaction. A series of gradient times were designed to explore the impact of the reaction time. It can be observed from Figure 3B that when the incubation time was 60 minutes, the fluorescence intensity reached a stable state. At the same time, four common buffer solutions of PB, PBS, Tris-HCl, and TE were selected, and their influence on the reaction was investigated. As shown in Figure 3C, when TE buffer was used, the fluorescence recovery value reached the maximum. In summary, 40°C, 60 minutes and TE buffer was the preferred reaction condition.

Figure 3A. Prioritization of the experimental environment. The effect of incubating temperature.

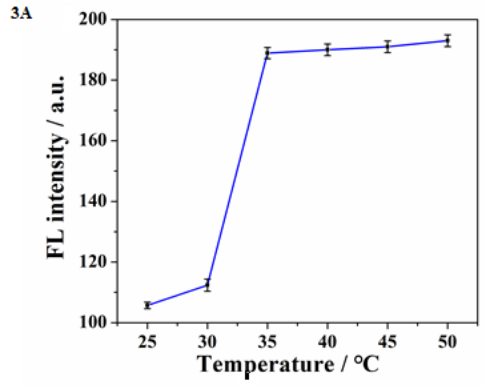

Figure 3B. Prioritization of the experimental environment. The effect of incubating time.

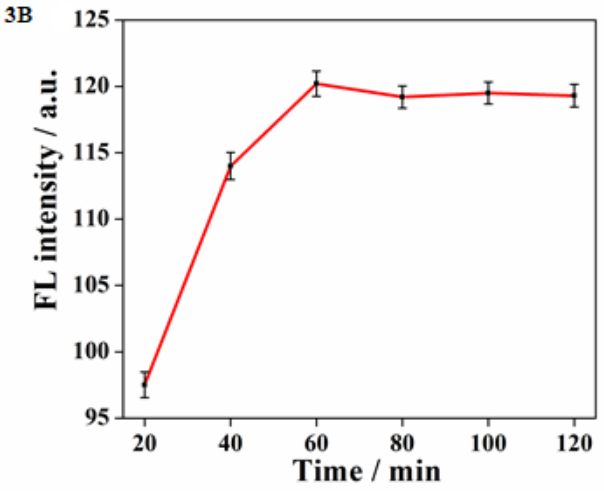

Figure 3C. Prioritization of the experimental environment. The effect of incubating buffer.

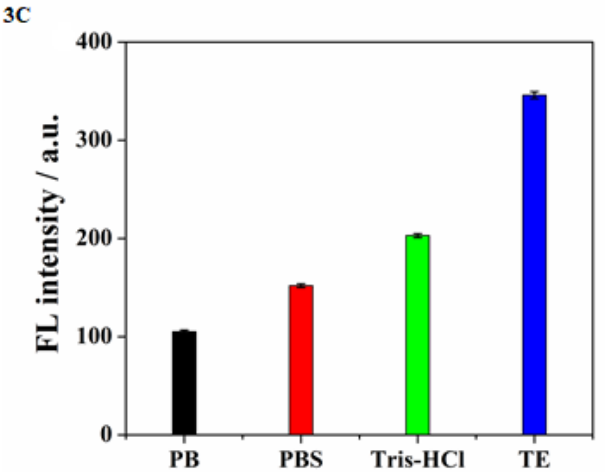

afld gene target and specificity analysis

NCQDs and AuNPs were used as fluorescence response signals and quenchers to design the fluorometric assay platform for the aflD genes detection. To evaluate the analytical performance of this method, diverse

concentrations of the aflD gene were measured ranging from 10 nM to 150 nM under the determined optimal experimental conditions. As shown in Figure 4A, with the increase of aflD gene concentration, the fluorescence signal gradually was increased. There was a positive linear correlation between F/F_0 and the aflD gene concentration in the range of 10 nM to 150 nM, where F_0 and F are the fluorescence intensity of NCQDs before and after quenching. The linear relationship of F/F_0 and aflD genes concentrations can be expressed as F/F_0=0.00519 c_{aflD}+0.97302, with R^2 = 0.996 (Figure 4B). The Limit of Detection (LOD) is 1.95 nM (3 σ /k) determined based on the equation. The specificity was other crucial feature for estimating analytical performance and was measured for the detection system. The column chart below exhibited the specificity of the provided detection method that was tested using AuNPs@Hairpin DNA-NCQDs to react with four kinds of DNA sequences, such as perfectly complementary target DNA, two-base mismatched DNA, five-base mismatched DNA, and Random DNA at the same concentration with the procedures of complementary DNA, respectively. The results were shown in Figure 4C. What was observed was that the detection system of perfectly complementary DNA for the hairpin probe showed the strongest fluorescence signal, which was ascribed to DNA base pairing to magnify the further distance between NCQDs and AuNPs. The fluorescence signal of the two-base mismatched and five-base mismatched DNA used target was altered slightly, compared with that of the blank control group. Furthermore, there was approximately no change in the fluorescence signal of Random DNA as analyte compared with blank control group. These consequences proved that the established fluorescence detection method has excellent sensitivity and specificity towards the aflD gene in examination system over other genes.

The feasibility of the constructed method in real samples

The feasibility of the designed strategy for the detection of the aflD gene was tested. The rice samples were contaminated in purpose. To ensure that *Aspergillus flavus* was produced on the rice samples, the *Aspergillus flavus* solution was evenly coated on the rice treated with sterile water. The rice samples were then incubated at 37 °C and water activity of 0.92 (a_w 0.92) for three days before use. Firstly, the DNA was extracted from *Aspergillus flavus* and *Aspergillus flavus*-contaminated rice by ezup column-based fungal genomic DNA extraction kit purchased from sangon (Shanghai, China). The obtained DNA used as template DNA for PCR amplification to obtain 76 bp DNA strand. PCR amplification of the 76-mer antisense strands of the aflD gene was carried out with a 20-mer forward primer and a 20-mer reverse primer. The specific parameter settings were referred to the literature [38]. The obtained DNA product was verified by using agarose gel electrophoresis and annealed at 95°C to free single-stranded DNA for next reaction. The PCR reaction of the alfD gene was shown in the Supplementary Figure 2B. The PCR product of *Aspergillus flavus* and *Aspergillus flavus*-contaminated rice is very consistent. Fluorescence DNA sensor was used to detect the PCR products of the 76-mer antisense strands of the aflD gene extracted from rice contaminated by *Aspergillus flavus*. The results were exhibited in Figure 4D and the DNA sensor blank control was also shown in the picture. By incorporating the PCR products of the aflD gene, the fluorescence intensity was elevated noticeably. This graph had uncovered that the obvious increase of fluorescence was contributed to the integration of the immobilized fluorescence probes to the PCR products of *Aspergillus flavus* from contaminated rice. In conclusion, the DNA concentration of the aflD gene was 69.75 nM. So far there is little information about DNA sensor for aflatoxin biosynthesis-related genes aflD, the reported methods were listed in Supplementary Table 1 [39,40].

Figure 4A. The sensitivity of aflD gene detection based on FRET and the fluorescence emission signal in the existence of different concentrates of aflD gene in the range of 0 nM-150 nM.

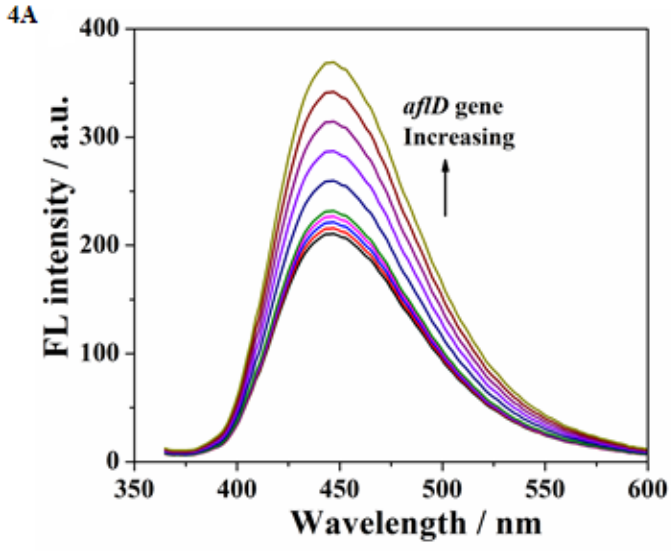

Figure 4B. The sensitivity of aflD gene detection based on FRET and the linear correlation between F/F_0 and the aflD gene concentration. **Note**: $Y=0.00519X+0.97302$; $R^2=0.9963$.

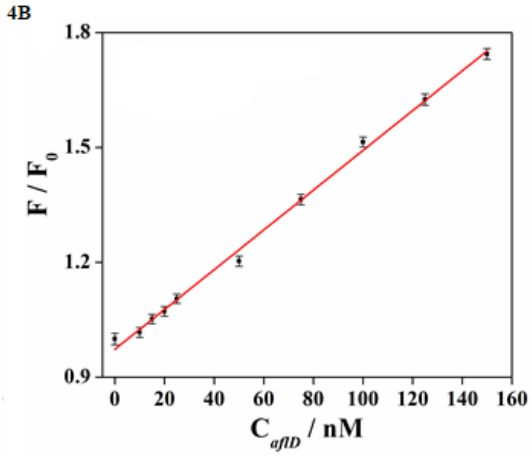

Figure 4C. Specificity and selectivity of the proposed method for target *aflD* gene (100 nM).

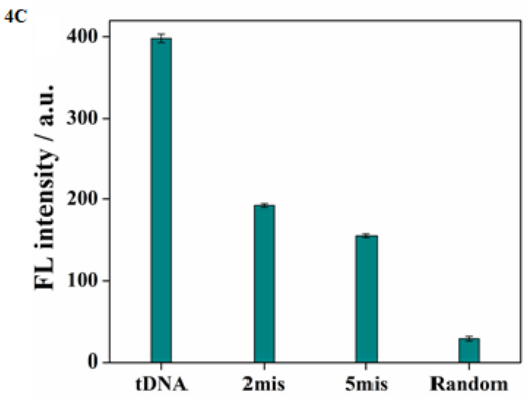

Figure 4D. FRET analysis of PCR product of contaminated rice (black curve: blank control, red curve: experimental control of PCR product of contaminated rice).

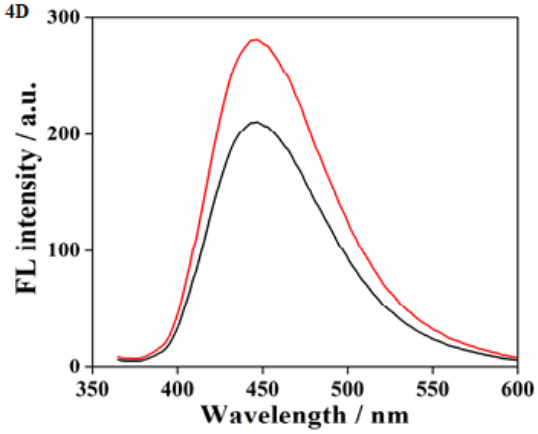

CONCLUSION

This fluorometric sensing system is composed of hairpin DNA functionalized NCQDs and AuNPs as fluorescence donor and acceptor. This biosensor offers a simple, rapid and sensitive method for detection of aflD gene, which benefit from unique nanostructure and optical properties of hairpin DNA, NCQDs and AuNPs. The microminiaturization of DNA fluorescence sensor established provides the possibility for on-suit, real-time and online detection of the aflD gene of *Aspergillus flavus*. Moreover, it has the advantage of low cost, no labeling, simple operation, and fast response speed. Due to the complexity and diversity of genes involved in toxins, the specificity of the method established in this study to detect toxin-producing bacteria needs to be further improved. In the future, some strategies such as nucleic acid signal amplification techniques and ratiometric fluorescence are supposed to take into consideration to solve this problem. This research on human pathogenic *Aspergillus*, the virulence and diversity of isolated bacteria in nature, and the research on gene function and diversity involved in toxin production still need to be enhanced.

AUTHORS CONTRIBUTIONS

Tao Yu: Methodology, Software, Investigation, Writing-original draft. Shuangfeng Peng: visualization. Qingyue Sun: visualization. Dezhao Kong: formal analysis. Chang Liu: data curation. Qiaoqiao Shi: formal analysis. Yaqi Li: supervision and writing guidance. Yong Chen: Writing-review and editing.

CONFLICTS OF INTEREST

The authors declare that they have no known competing financial interests or personal relationships that could have appeared to influence the work reported in this paper.

FUNDING

This work was supported by the National Natural Science Foundation of China [No. 31901799, 32001804]. This work was supported by the China Postdoctoral Science Foundation (No. 2021M692370). This work was supported

by the Emerging science and technology innovation team funding of JUST (No. 1182921902). This work was supported by the Dual creative talents program of Jiangsu province (Grant No. 1184902001). This work was supported by the Research start-up fund of Jiangsu University of science and technology (Nos. 1182932001, 1182922001).

DATA AVAILABILITY STATEMENT

The data used to support the findings of this study are available from the corresponding author upon request.

ACKNOWLEDGEMENT

This work was financially supported by the National Natural Science Foundation of China (No. 31901799, 32001804), China Postdoctoral Science Foundation (No. 2021M692370), Emerging science and technology innovation team funding of JUST (No. 1182921902), Dual creative talents program of Jiangsu province (Grant No. 1184902001), Research start-up fund of Jiangsu University of science and technology (Nos. 1182932001, 1182922001)

REFERENCES

1. Hou Y, et al. Aptasensors for mycotoxins in foods: Recent advances and future trends. Compr Rev Food Sci F. 2022;21:2032-2073.
2. Deng R, et al. Recognition-enhanced metastably shielded aptamer for digital quantification of small molecules. Anal Chem. 2018;90:14347-14354.
3. Ma S, et al. Using magnetic multiwalled carbon nanotubes as modified QuEChERS adsorbent for simultaneous determination of multiple mycotoxins in grains by UPLC-MS/MS. J Agric Food Chem. 2019;67:8035-8044.
4. Claeys L, et al. Mycotoxin exposure and human cancer risk: A systematic review of epidemiological studies. Compr Rev Food Sci F. 2020;19:1449-1464.
5. Bhat R, et al. Mycotoxins in food and feed: Present status and future concerns. Compr Rev Food Sci F. 2010;9:57-81.
6. Scherm B, et al. Detection of transcripts of the aflatoxin genes aflD, aflO, and aflP by reverse transcription-polymerase chain reaction allows differentiation of aflatoxin-producing and non-producing isolates of *Aspergillus flavus* and *Aspergillus parasiticus*. Int J Food Microbiol. 2005;98:201-210.
7. Zhou R, et al. Enzymatic Function of the Nor-1 Protein in aflatoxin biosynthesis in *Aspergillus parasiticus*. Appl Environ Microbiol. 1999;65:5639-5641.
8. Dalie DKD, et al. Lactic acid bacteria-potential for control of mould growth and mycotoxins: A review. Food Control. 2010;21:370-380.
9. McGrath TF, et al. Biosensors for the analysis of microbiological and chemical contaminants in food. Anal Bioanal Chem. 2012;403:75-92.

10. Ardakani MM, et al. Sex determination based on amelogenin DNA by modified electrode with gold nanoparticle. Anal Biochem. 2013;443:132-138.

11. Meng Q, et al. Highly photoluminescent carbon dots for multicolor patterning, sensors, and bioimaging. Angew Chem Int Ed. 2013;52:3953-3957.

12. Huang S, et al. A ratiometric nanosensor based on fluorescent carbon dots for label-free and highly selective recognition of DNA. RSC Advances. 2015;5:44587-44597.

13. Bonis-O Donnell JTD, et al. A universal design for a DNA probe providing ratiometric fluorescence detection by generation of silver nanoclusters. Nanoscale. 2016;8:14489-14496.

14. Zhang L, et al. Simultaneous determination of protein kinase A and casein kinase II by dual-color peptide biomineralized metal nanoclusters. Analy Chem. 2016;88:11460-11467.

15. Wang L, et al. Simultaneous quadruple-channel optical transduction of a nanosensor for multiplexed qualitative and quantitative analysis of lectins. Chem Commun. 2018;54:7754-7757.

16. Tian J, et al. Fluorescence resonance energy transfer aptasensor between nanoceria and graphene quantum dots for the determination of ochratoxin A. Analytica Chimica Acta. 2018;1000:265-272.

17. Zhao Y, et al. Ochratoxin A detection platform based on signal amplification by exonuclease III and fluorescence quenching by gold nanoparticles. Sens Actuators B. 2018;255:1640-1645.

18. Shi J, et al. Nanoparticle based fluorescence resonance energy transfer (FRET) for biosensing applications. J Mater Chem B. 2015;3:6989-7005.

19. Forster T. Intermolecular energy migration and fluorescence. Ann Phys. 1948;437:55-75.

20. Xu W, et al. A homogeneous immunosensor for AFB_1 detection based on FRET between different-sized quantum dots. Biosens Bioelectron. 2014;56:144-150.

21. Gao PF, et al. Plasmonics-attended NSET and PRET for analytical applications. TrAC Trends Anal Chem. 2020;124:115805.

22. Hu J, et al. Integration of isothermal amplification with quantum dot-based fluorescence resonance energy transfer for simultaneous detection of multiple microRNAs. Chem Sci. 2018;9:4258-4267.

23. Liu J, et al. Carbon dots: A New Type of carbon-based nanomaterial with wide applications. ACS Cent Sci. 2020;6:2179-2195.

24. Tyagi S, et al. Multicolor molecular beacons for allele discrimination. Nat Biotechnol. 1998;16:49-53.

25. Liu Y, et al. J-aggregate-based FRET monitoring of drug release from polymer nanoparticles with high drug loading. Angew Chem Int Ed. 2020;59:20065-20074.

26. Cui L, et al. Advances in the integration of quantum dots with various nanomaterials for biomedical and environmental applications. Analyst. 2018;143:2469-2478.

27. Liu M, et al. A fluorometric aptamer-based assay for ochratoxin A by using exonuclease III-assisted recycling amplification. Microchim Acta. 2019;187:46.

28. Liu ML, et al. Carbon dots: Synthesis, formation mechanism, fluorescence origin and sensing applications. Green Chem. 2019;21:449-471.

29. Xu S, et al. Polydopamine nanosphere/gold nanocluster (Au NC)-based nanoplatform for dual color simultaneous detection of multiple tumor-related MicroRNAs with DNase-I-assisted target recycling amplification. Anal Chem. 2018;90:4039-4045.

30. Li Y, et al. A novel fluorescent fret hairpin probe switch for aflD gene detection in real fermented soybean paste. Food Anal Methods. 2021;14:2469-2477.

31. Sheng A, et al. MXene coupled with CRISPR-Cas12a for analysis of endotoxin and bacteria. Anal Chem. 2021;93:4676-4681.

32. Hildebrandt N, et al. Energy transfer with semiconductor quantum dot bioconjugates: A versatile platform for biosensing, energy harvesting, and other developing applications. Chem Rev. 2017;117:536-711.

33. Grabar KC, et al. Preparation and characterization of Au colloid monolayers. Anal Chem. 1995;67:735-743.

34. Liu J, et al. Preparation of aptamer-linked gold nanoparticle purple aggregates for colorimetric sensing of analytes. Nat Protoc. 2006;1:246-252.

35. He JH, et al. Carbon dots-based fluorescence resonance energy transfer for the prostate specific antigen (PSA) with high sensitivity. Talanta. 2020;219:121276.

36. Xu J, et al. Nanocomposites of graphene and graphene oxides: Synthesis, molecular functionalization and application in electrochemical sensors and biosensors. A review. Microchim Acta. 2017;184:1-44.

37. Gui R, et al. DNA assembly of carbon dots and 5-fluorouracil used for room-temperature phosphorescence turn-on sensing of AFP and AFP-triggered simultaneous release of dual-drug. Sens Actua B. 2018;255:1623-1630.

38. Khavidak SS, et al. Detection of aflD gene in contaminated pistachio with *Aspergillus flavus* by DNA based electrochemical biosensor. J Food Prop. 2017;20:S119-S130.

39. Yu J, et al. Comparative mapping of aflatoxin pathway gene clusters in *Aspergillus parasiticus* and *Aspergillus flavus*. Appl Environ Microbiol. 1995;61:2365-2371.

40. Zhang H, et al. Simultaneous determination of concanavalin a and peanut agglutinin by dual-color quantum dots. Analy Chem. 2013;85:10969-10976.